Acoustic intensity technique applied to monitor planetary gears

P. Garcia Fernandez, Ana de-Juan,
A. Diez-Ibarbia, J. Sanchez-Espiga, A. Fernandez del Rincon

Condition monitoring of gear trains by classic techniques based on vibrations and/or extensometry measurements requires the preparation of the sensor contact surfaces and the cables installation. In the case of planetary gear trains, this task is more difficult due to their compactness and the complexity of the relative movements among their different elements. As an alternative, the authors studied the possibility of using acoustic measurements for the planetary gear-set characterisation, as well as for predictive maintenance of this mechanical system. In order to perform this study, a suitable measurement equipment was selected and a bespoke software was developed to control it, to process the data, as well as to represent the results. This informatic tool was used to perform the acoustic characterisation, in which acoustic pressure and intensity measurements were combined with advanced algorithms, such as sincronous-average technique. In this study, two different failures were experimentally recreated in a commercial gearbox, representing the results by frequency and order spectra and intensity maps. The obtained results were compared with those obtained in the box without defect.

1. Introduction

Gear transmission systems are critical components in many industrial applications (power generation, automobiles, agricultural and construction machinery, helicopters, etc.) [1-4]. In consequence, the reliability requirements for this type of elements are increasing every day, both due to the economic costs and to the human life risk, to which a system failure can lead [5-10].

In the last decades, the use of planetary gear trains has increased due to their compactness and lightness, especially when high-torque levels and/or high transmission ratios are involved. The increase in their use has been accompanied by more demanding technical requirements and has led to the need for improving their design, and more specifically, their reliability. Although the vibration sources for planetary gears are the same as in fixed-axe trains, planetary gears have unique features which add complexity to the problem. Regarding this aspect, many researchers have developed models, both theoretical and experimental, in order to predict and optimize their dynamic behaviour under different operating conditions [11-13]. Likewise, several experimental techniques have been proposed, mainly focused on both the theoretical model validation and the development of predictive maintenance techniques for this mechanical system [14-16].

Its compactness implies important difficulties in monitoring this kind of gears by means of vibration and/or strain gauges measurements. Specifically, the sensors installation inside the train and their wiring are hampered by the scarce free volume in its interior and by the complex relative movement among its components. Even the use of telemetry systems instead of wires and slip rings is not always a valid solution. Among other drawbacks, its use implies the modification of the mass of the systems and the possible introduction of unbalances. The installation of external sensors is simpler but needs a contact with the device and requires space, which sometimes is unavailable.

The present work aims to offer an alternative to the abovementioned methods, by using acoustic measurements for condition monitoring [17-20] and its application to predictive maintenance. For the sake of simplicity and in order to offer a competitive alternative, acoustic characterization proposed in this paper is developed by measuring sound intensity [21-22] and pressure. With this approach, the sensors can be placed in an easier and quicker way and, more importantly, they do not need to be in contact with the components. To guarantee the success of the procedure, it is vital that the acoustic surrounding of the system remains approximately stable, which makes it suitable for a wide range of applications, from monitoring a wind turbine gearbox inside its nacelle to control quality in a gearbox assembly line. In order to achieve this goal, a set of measurements were developed in a planetary test bench [23].

In order to validate the proposed acoustic technique, it has been used to characterise the behaviour in operation of a specific planetary test bench, which were previously developed by the authors, extensively presented in the

literature [23-25] and summarised in section 2 for the sake of simplicity. The proposed acoustic technique is detailed in the third section. In section 4, the characterisation results are shown when this acoustic technique is used in a perfectly lubricated gear set, and then compared with those obtained in presence of defects (no lubrication and a notch on the tooth root), which are presented in section 5. Finally, some conclusions of the study and references are detailed in sections 6 and 7.

2. Test Bench set-up

The test bench used in this work was previously designed and built by the research team [23-25] in order to experimentally validate an advanced computational model of planetary gear transmissions. It is a back-to-back configuration (Fig. 1) with a mechanical power recirculation composed by two identic planetary stages with a sun, three planets, a ring and a carrier each. The teeth number of the sun, planets and ring is respectively 16, 24 and 65. One of the stages is the test specimen, where the ring is fixed, whilst the other only acts as an auxiliary system, which enables the power recirculation by means of a free ring. The load on the gears is introduced by means of weights connected to the ring of the auxiliary train through a lever. The movement of the whole system is produced by an electric motor, which only has to provide the test bench power losses.

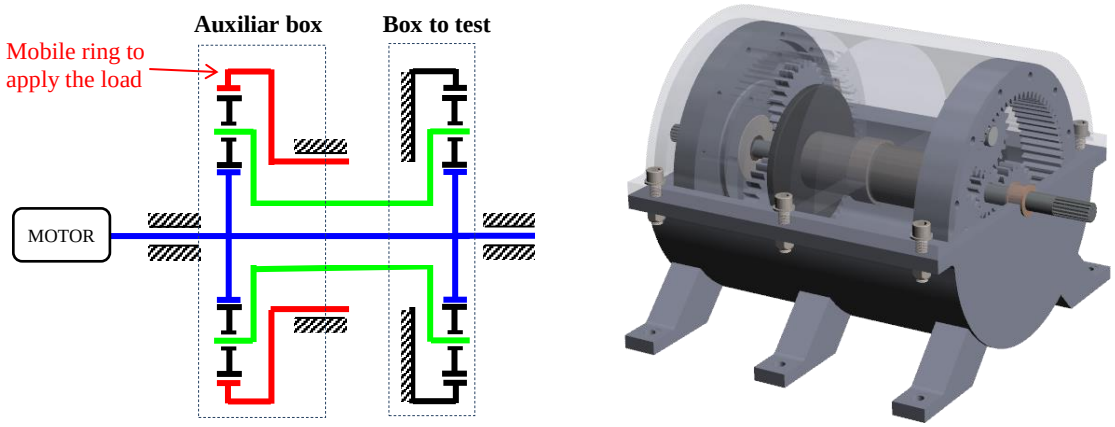

Fig. 1. Mechanical scheme and CAD model of the test bench.

In order to achieve the mechanical power recirculation, it is necessary to connect the carriers and the suns of both trains (Fig. 1). Given the concentricity of both elements, a hollow shaft is used to connect the satellite carriers, whilst the shaft which connects the suns is housed inside the hollowed one. This configuration is very compact, but makes very difficult to install internal sensors and wiring. In some cases, it is necessary to make through holes and the use of slip rings. A picture of the actual system is shown (Fig. **2**)

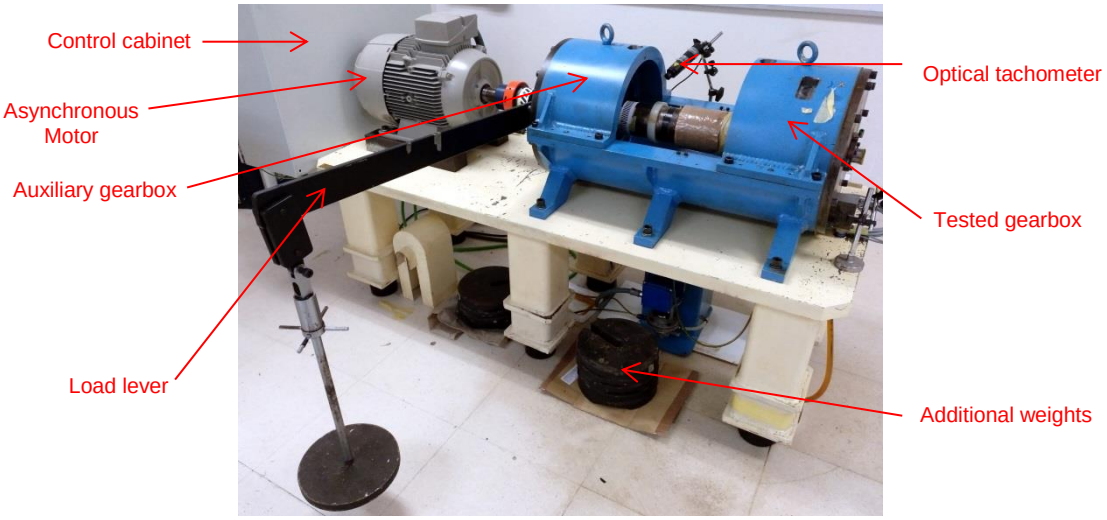

Fig. 2. Actual test bench.

3. Mesaurement tool developed to perform the acoustic characterisation

One of the main tasks of this work was the development of a unified computer tool which allows for the measurement control, the treatment of the registered data and the representation of the resultant parameters. The Matlab® environment was chosen as programming platform for this tool due to its built-in powerful routines of application in each of the aforementioned aspects. The measuring chain that controls the computer tool consists of the following elements: Intensity probe (type-2 microphones + solid spacer), multichannel signal analyser and optical tachometer (Table 1).

It should be noted that, although several hardware-software sets were available for the measurements, most of them did not have all the required processing options or did not allow for a custom representation of the results. Therefore, an acquisition NI USB-9233 card was finally chosen. This card could be completely controlled from Matlab through the Data Acquisition Toolbox. In addition to the development of mathematical algorithms, such as the calculation of sound intensity, FFT, synchronous averaging, etc., the choice of this hardware forced the development of additional functions for the configuration of hardware parameters, the control of the acquisition process and signal storage. Besides unifying and controlling all operations, this solution provides the possibility of future expansion by, for example, integrating an automated diagnosis system.

Table 1. Description of the main instrumentation used.

Equipment type	Model	Description
Sound intensity probe	Brüel & Kjær Type 3595	2 microphones, 12mm solid spacer
Data acquisition device	NI USB-9233	50 KS/s per channel, 4 channels 24 bits, 120 dB dynamic range.
Optical tachometer	Compact instruments VLS7/T/LSR+ Striped tape	100 pulses/rev.

The software developed can be grouped into three different but interrelated modules: acquisition, processing and representation modules. All of them have a graphical user interface for a quick and convenient use. The acquisition module has two measurement options: one for the measurement at each point of the reference grid with constant value of load and speed, and another for the acquisition at a single point of measurement when different levels of load and speed are applied. The first option allows for the subsequent elaboration of intensity maps, acoustic source location, calculation of the power radiated by a face, etc. whilst the second one enables the study of the test bench for different operating regimes. Both options contemplate the following steps: 1. Checking and configuration of the hardware, 2. Measurement chain calibration, 3. Determination of the carrier speed rotation, 4. Grid, load and speed specification, 5. Acquisition and recording of microphone and tachometer signals.

The fact of having associated the tachometric signal to the sound pressure of the two microphones allows for performing multiple types of analysis. Some advanced analysis routines have been implemented within the processing module, both for the characterisation of the rig and for the detection of failures. These functions are: Temporary synchronous averaging, temporary synchronous averaging with data overlap, intensity spectrum in 1⅓ octave for all angular positions and synchronous averaging in frequency.

Finally, with regard to the representation module, different functions were created to represent the processed data. These routines allow, among others, to obtain intensity maps (both in contour lines and in coloured strips), either for all the thirds of an octave in a certain position of the gear train or for a complete spin in a specific third of an octave. It is possible to visualise the results through films which show the transition among different maps, as well as to obtain spectrum representations in frequency domain at each grid point of acoustic pressure and intensity.

4. Test bench acoustic charaterisation

In order to perform the acoustic characterization of the test bench without defects, both intensity and sound pressure measurements were carried out for different operating conditions. For this purpose, 9 load levels were established from 200 Nm to 1800 Nm (besides the level 0 which represents idle conditions) and 3 motor speeds: 300, 600 and 900 rpm. These values were considered to be representative of the potential operating conditions to which the gear train will be subjected in its actual application. The measurement campaign was carried out mainly in two perpendicular planes of the rig for each combination of load-speed values: parallel to the front face and to its side face respectively (Fig. 3). Once the data of the measurement campaign was acquired and recorded, its processing was focused on the following aspects: Identification of mesh frequencies by means of

acoustic pressure and intensity spectra, representation of acoustic intensity maps and films creation of acoustic intensity maps.

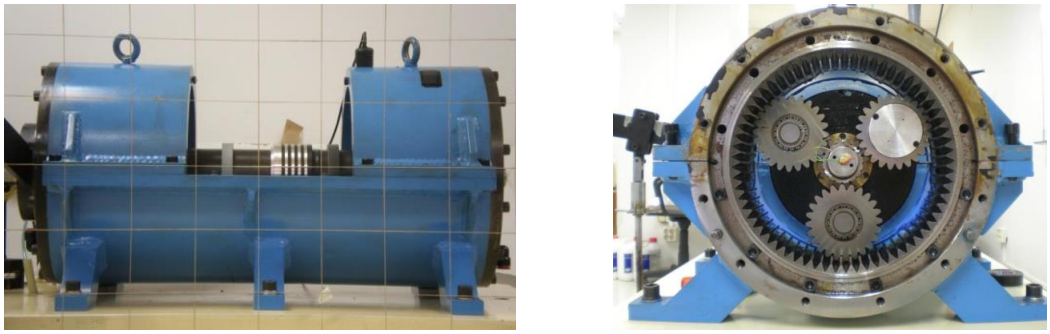

Fig. 3. Front face (with reference grid) and side face (without cover) in the starting angular position.

To identify the meshing frequencies, measurements were made for two specific positions of the probe: one inside and another outside the bench housing. The first one is located between the two planetary boxes, orienting the intensity probe to the test train at a radial position coincident with the planets pin trajectory. The noise coming from the other gear train was decreased through a cover of acoustic material. The outer measuring point is located on the side face, also at the same radius of the planets pin trajectory. In this case, an acoustic enclosure of the test bench excepting for the side face were made (Fig. 4)

Next, the results in terms of acoustic pressure and intensity spectra are presented in the aforementioned points, when there is no defects and the test bench is perfectly lubricated. Specifically, only the results of three torque levels (level 3, 6 and 9, which correspond to 600Nm, 1200Nm and 1800Nm) are shown in the three considered speed conditions for the sake of brevity. First, the inside point results are assessed in terms of global noise and orders of the carrier rotational speed, following with the same analysis of the outside point, and finally, the intensity maps of the front an lateral faces are presented for different frequencies and positions, using the synchronous averaging processing (TSA) technique.

Fig. 4. Inside and outside points of measurement and acoustic test bench housing.

The meshing is considered as the main excitation source of the system under normal conditions. According to its kinematic parameters, the characteristic frequencies of the gearbox for each test speeds are those shown in Table 2.

Table 2. Characteristic frequencies of the planetary gearbox for each test speeds

N_s (rpm)	f_s (Hz)	f_m (Hz)	f_c (Hz)	f_p (Hz)
300	5	64,20	0,99	2,67
600	10	128,40	1,98	5,35

Where fs, fm, fc and fp means the rotational frequencies of the sun, mesh, carrier and planet respectively.Moreover, from and experimental modal analysis, the first twenty natural frequencies of the test bench were determined. These are: 76, 136, 169, 195, 251, 301, 325, 352, 378, 406, 436, 466, 526, 558, 578, 604, 687, 755, 783, 803 Hz.

4.1. Inside point results

First, the global noise spectra are shown (Fig. 5). Although the acoustic intensity spectra are shown in the same range as the pressure ones, they are only valid between 125 and 5000 Hz due to the spacer used.

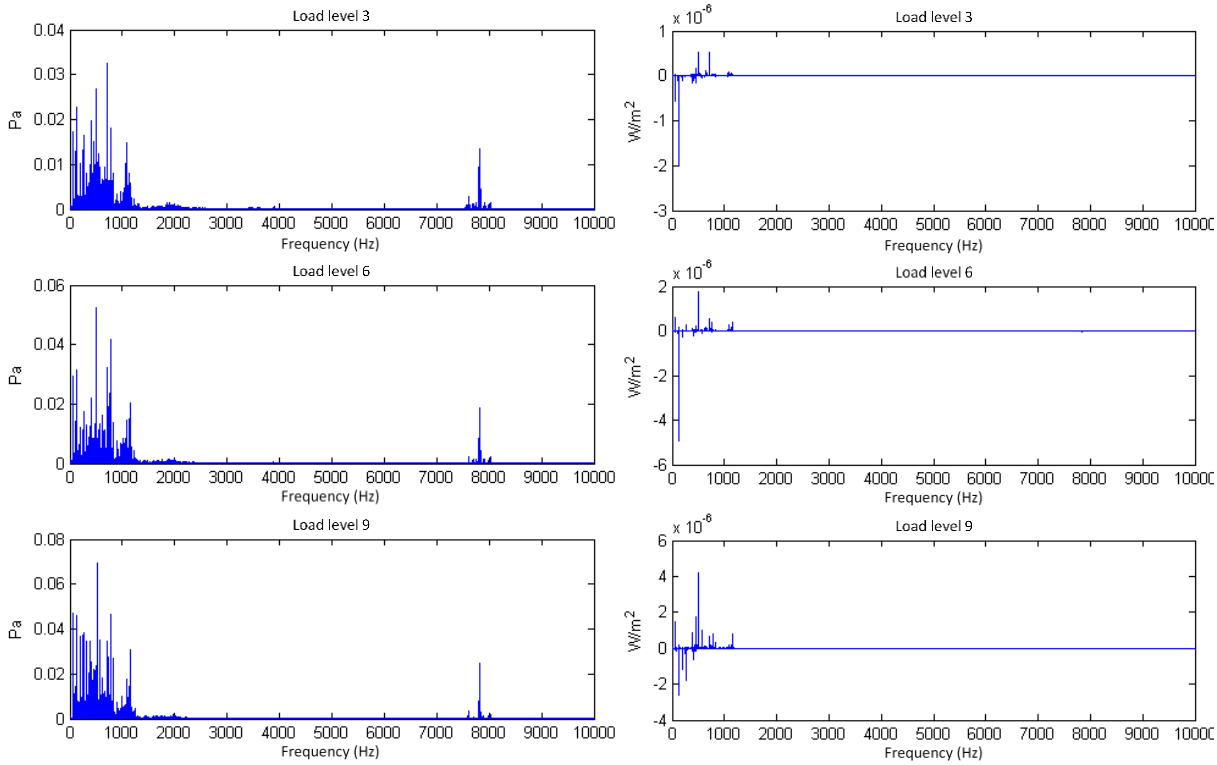

Fig. 5. Acoustic pressure and intensity spectra on the inside point (Speed 1).

It can be noticed the following facts:

- The general shape of the acoustic pressure spectra remains constant for the different load levels and, as the load increases, so does the acoustic pressure magnitude in an almost proportional way. This behaviour is expected in a gear train which correctly operates.
- A peak appears at approximately 8 kHz, as well as their respective sidebands, in pressure spectra of all load levels. Although it increases with the load, it does so in a smaller proportion than the rest of the spectrum. This fact, together with its high frequency, seems to indicate that said peak does not come from a mechanical element of the test bench.
- In the intensity spectra, an increase in amplitude is also seen with the load level.

The results, in terms of order with respect to the carrier rotational speed, are shown next. The order number is limited to the range in which the frequency of the gear and its multiples are expected to be found. The acoustic pressure and intensity for the first considered speed are shown in Fig. 6.

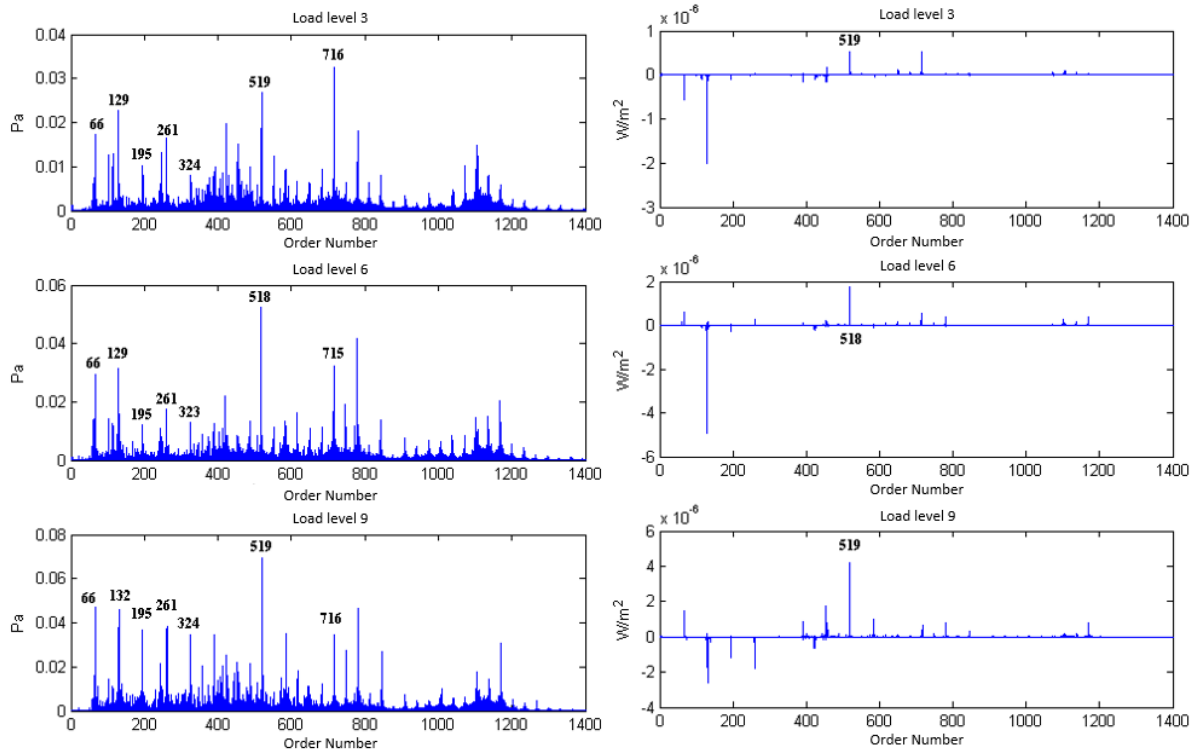

Fig. 6. Acoustic pressure and intensity spectra in orders on the inside point (speed 1).

The mesh frequency has a theoretical order number with respect to the carrier speed of 65. This order and its multiples appear clearly in the pressure order spectra. In addition, as the load increases, so does the magnitude of the peaks.

On the other hand, the intensity spectra do not provide as much information as the pressure ones. This is due to the complexity of the sound field around the probe. Consequently, only the pressure spectra for speed values 2 and 3 are presented in Fig. 7.

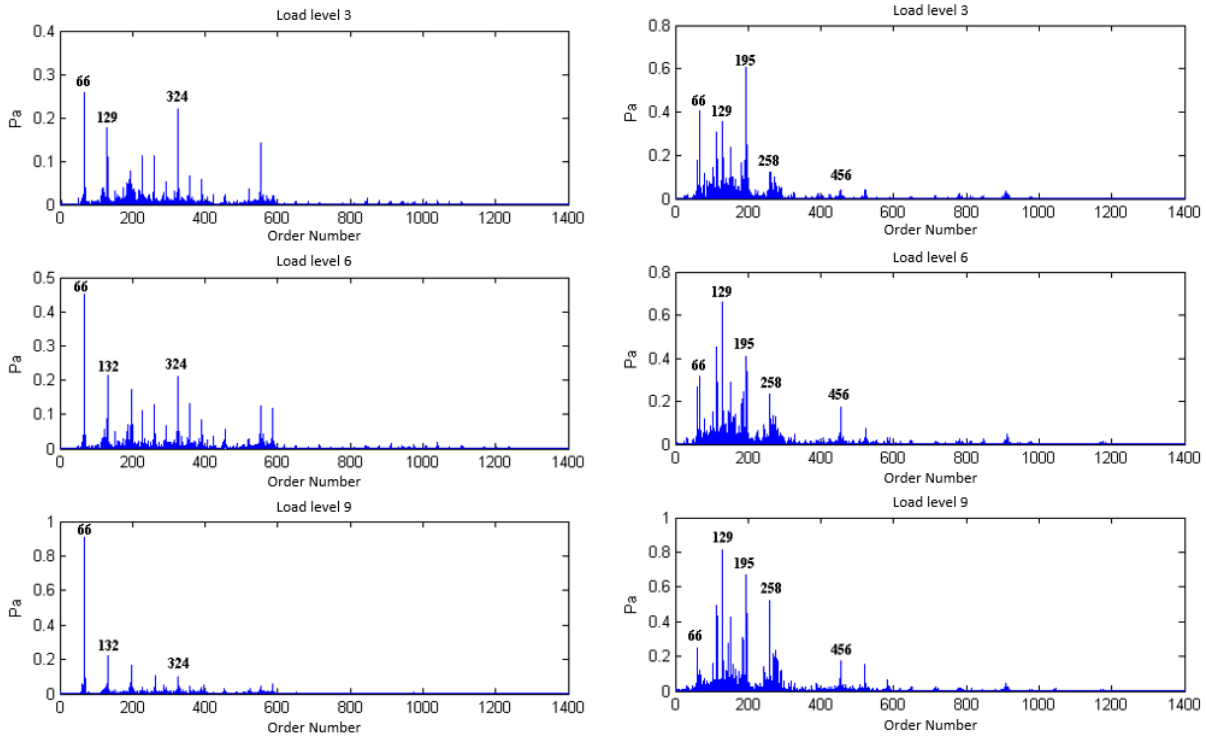

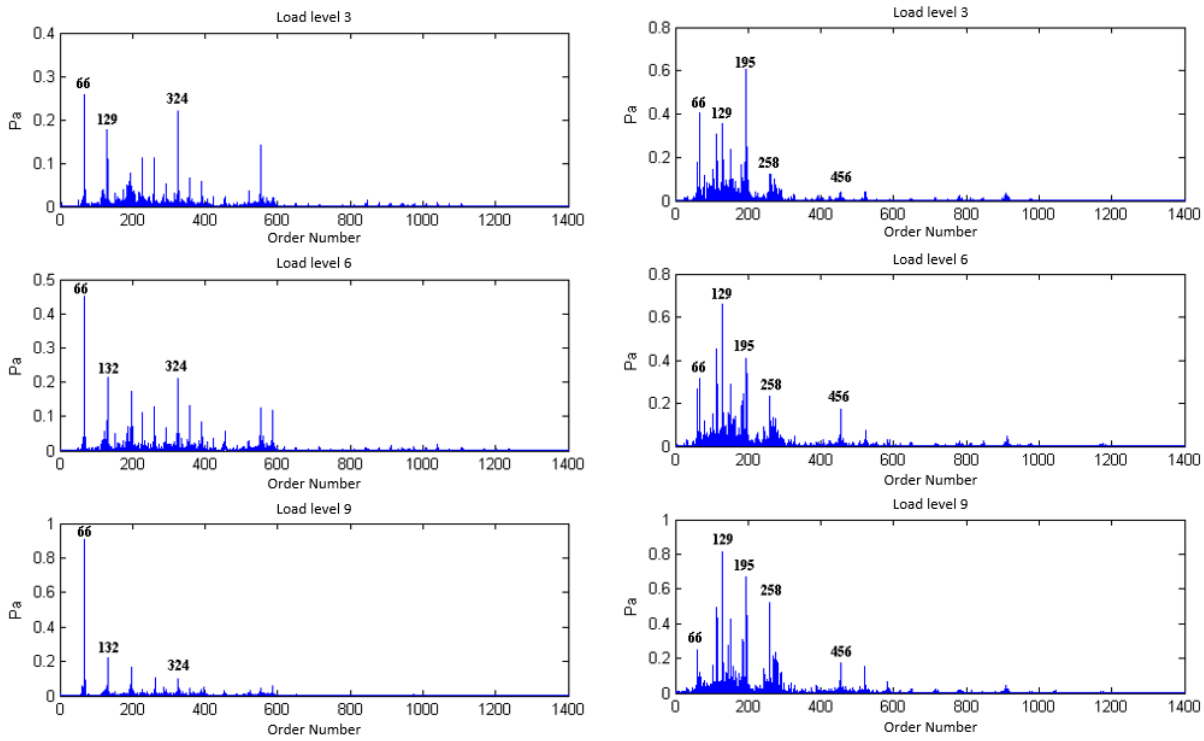

Fig. 7. Acoustic pressure spectra in orders on the inside point (Speed 2 on the left and 3 on the right).

It can be observed that:

- For a given speed, the spectrum keeps the shape although the amplitude values increase almost proportionally with the load.
- The spectra change completely when the speed varies: As the speed increases, the energy of the spectrum moves towards low frequencies.

4.2. Outside point results

For the measurement point located on the outside of the rig, the same representations were made as for the interior point. In this case, unlike the previous one, the acoustic intensity measurements are more significant: they show peaks corresponding to mesh frequencies and there are hardly negative values (Figure 7).

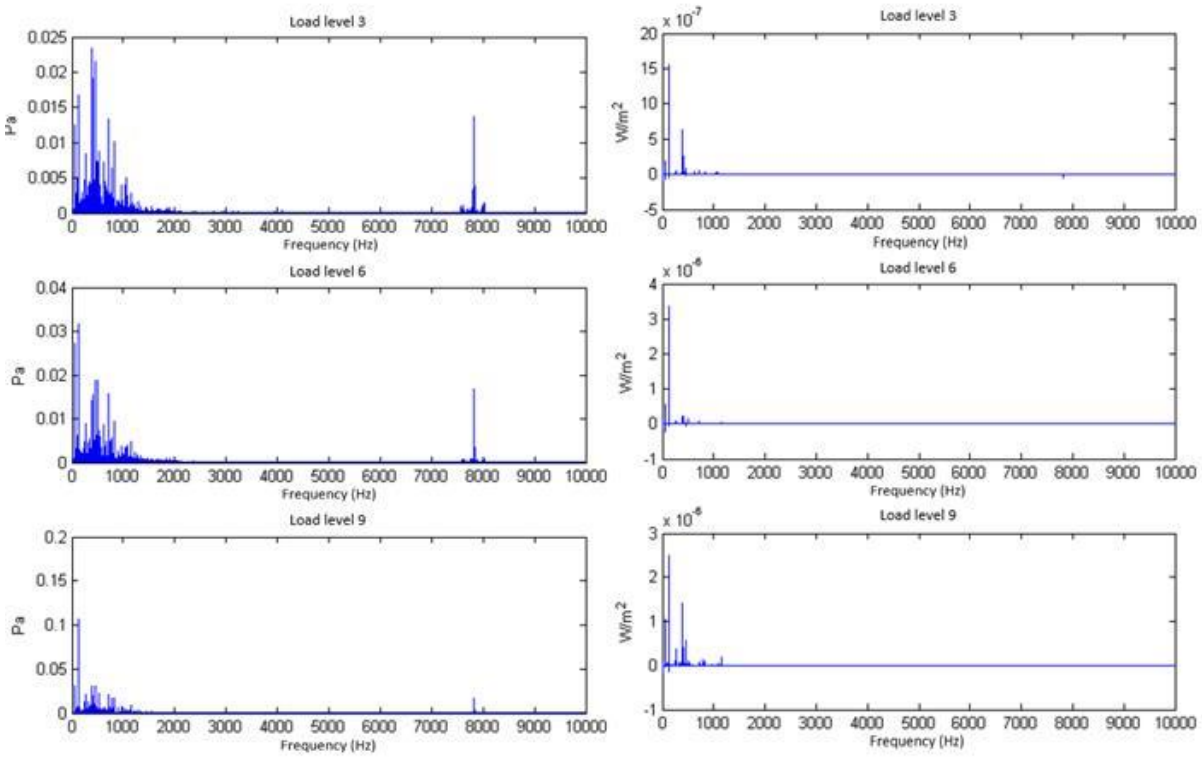

Fig. 8. Acoustic pressure and intensity spectra, outside point, speed 1.

In Fig. 8, the same point spectra are represented but applying synchronous averaging technique. This processing tool attempts to eliminate those components in frequency which are not in synchronism with the carrier rotation.

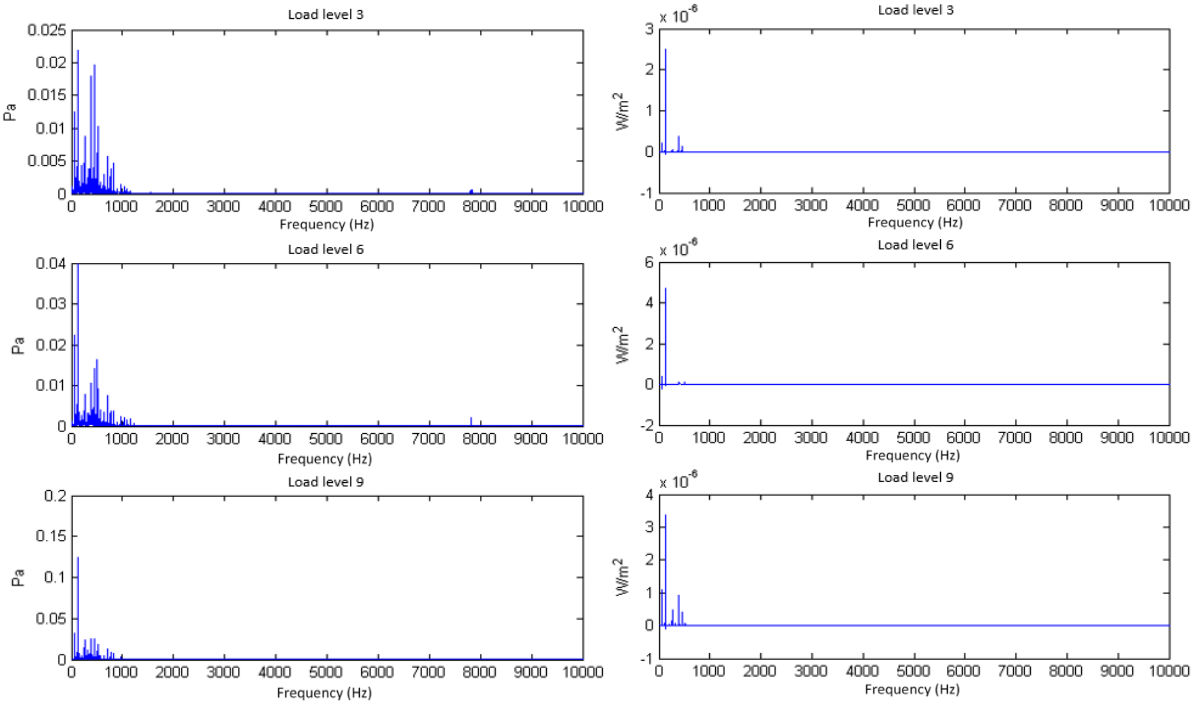

Fig. 9. Acoustic pressure and intensity spectra, outside point, synchronous averaging, speed 1.

After the study of the obtained spectra with synchronous averaging and their comparison with those obtained without its application, the following conclusions were obtained:

- In the global pressure spectrum, the 8 kHz harmonic and its sidebands were eliminated. This corroborates that this noise did not come from the test bench. After a subsequent process of locating sources, it was concluded that it came from the motor.
- Both pressure and intensity spectra appear more defined, besides, the components which are not coherent with the rotation carrier speed are attenuated.

4.3. Acoustic intensity maps

Two types of intensity maps series have been generated to locate and to quantify the sound sources at different operating conditions. Both types can be combined with the synchronous averaging processing (TSA) option or not. The first type consists of one map for every third octave band averaged over a whole spin of a gearbox. The second type series is for and specific third octave and consists of twelve maps, one for every sector of a spin. It should be noted that the postprocess module can combine the acoustic intensity maps into a film to make easier their interpretation.

As an example of the first type with TSA, two series of maps are shown (Fig. 10). They belong to the said frontal and lateral faces of the test bech operating under normal conditions. The values shown on the axes of figure 9 refer to the positions of the reference grid used in the intensity measurements. For the maps relative to the front face, the separation between consecutive points is 10 cm in both axes, and the coordinates (5,3) correspond to the midpoint between the two gearboxes. For the side face maps, the distance between consecutive positions is 5 cm on both axes. The coordinate (5,5) corresponds to the center of the the planetary gearbox face.

In the maps of the front face, it is observed that the highest sound levels appear in the upper central part for most frequency bands.This was expected as the rig is open in that region. This face does not show any meaningful pattern in the aera of the test box (right).

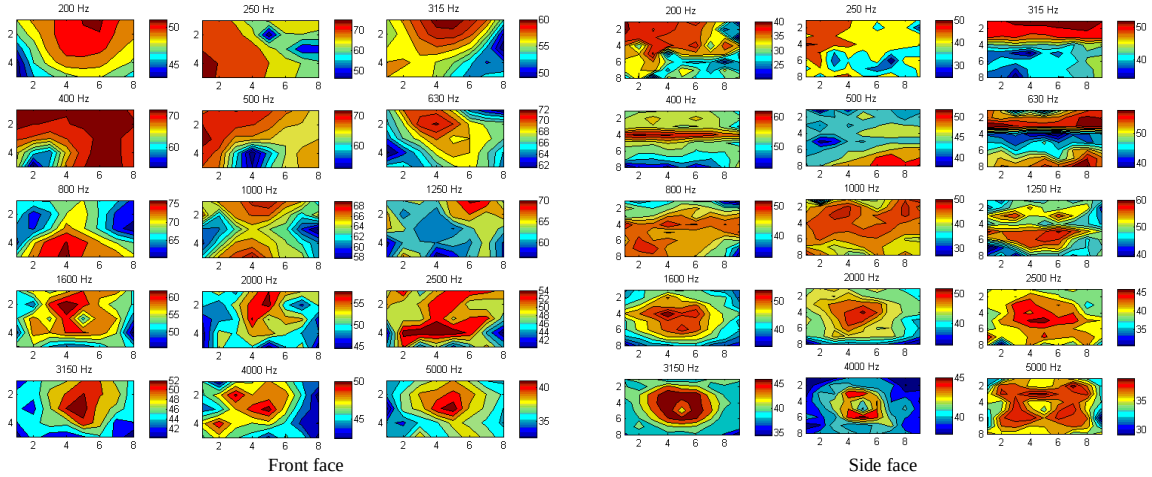

Fig. 10. Acoustic intensity maps of the front and side face, (Speed 2, Load 3, normal operation conditions).

Regarding the measurements on the side face, a circular pattern appears on the intensity maps from 1.6 kHz band. This pattern is according to the geometry of the planetary train and is more noticeable in high frequencies.

For the 3150 Hz band, a type 2 intensity map series is shown (Fig. 11). Although its sequencing in film can make it more evident, the planet movements can be observed through these maps.

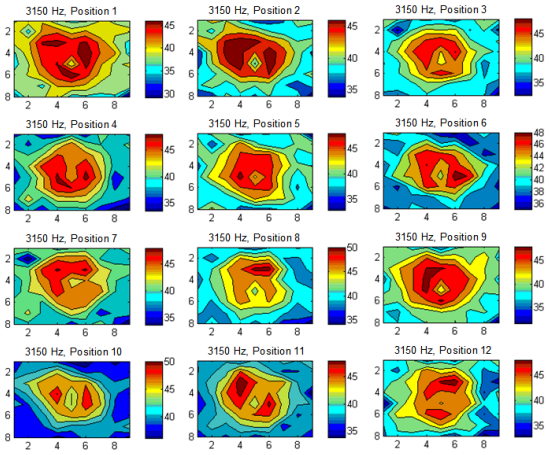

Fig. 11. Acoustic intensity maps of the side face for 12 positions/spin (3150 Hz, Speed 2, Load 3).

In the position 1 of Fig. 10, the center of the reference planet is just below the centre of the sun. The following positions correspond to successive increases of pi/6 radians counter clockwise with respect to the first one. Even in the presence of the gearbox side face cover, the maximum values of the acoustic intensity are found in the place occupied by the planets in each position. As it can be seen, there are no relevant differences among intensity levels in each position, as it could be expected from a planet without defects. The differences in the shape of the measurements in each position are due to different reasons: the test bench is not symmetric and the non-ideal acoustic conditions of the room. However, as these conditions remains, the intensity maps keep valid for comparison with those obtained for a defective gearbox.

5. Maintenance application

Once the acoustic characterization of the test bench was carried out, the application of the tool in the predictive maintenance of gears were assessed. In order to check the validity of these techniques in maintenance applications, two different tests were performed. In the first, a run-out of lubrication was reproduced in the test bench, whilst, in the second, a defective planet was incorporated.

5.1 Lack of lubrication test

In this test, a failure due to lack of lubrication was recreated (turning off the oil pump and cleaning the remaining oil in the gearbox) and a measurement campaign were performed under the same operating conditions used in the previous characterization. In this way, the results of both measures can be compared (Fig. 12). Only intensity maps of the lateral side are shown because they are more significant in this study than those obtained at the front face.

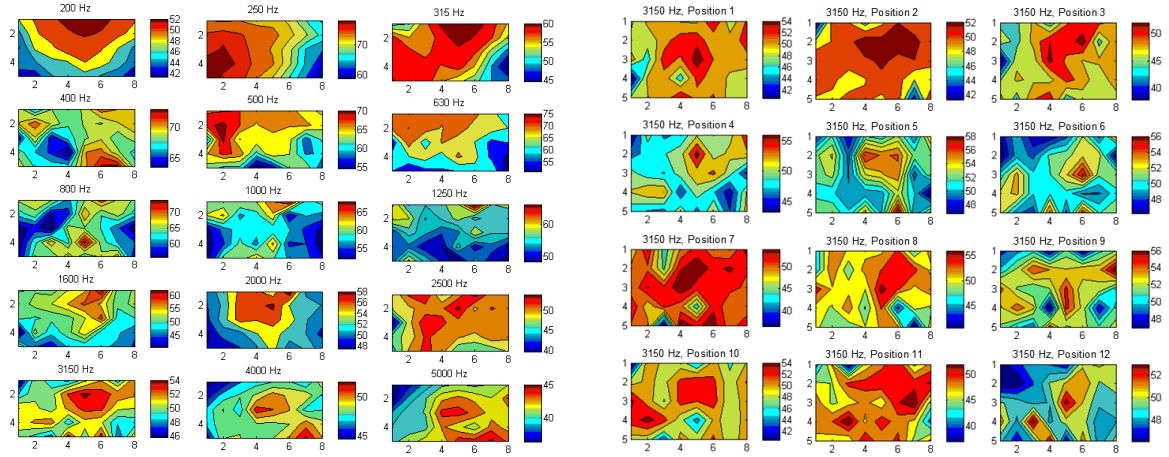

Fig. 12. Acoustic intensity maps of the side face in frequency bands and acoustic intensity maps of the side face for 12 positions/spin for 3150 Hz band (TSA, 3150 Hz, Speed 2, Load 3, no lubrication condion)

It is observed that the acoustic intensity values are greater in all the maps in this case than their respective ones with lubrication. Unlike the planetary train without defects, in this case the planets configuration cannot be observed.

Finally, the intensity spectrum is shown for the central grid position both under normal operating conditions and under operation without oil (Fig. 13).

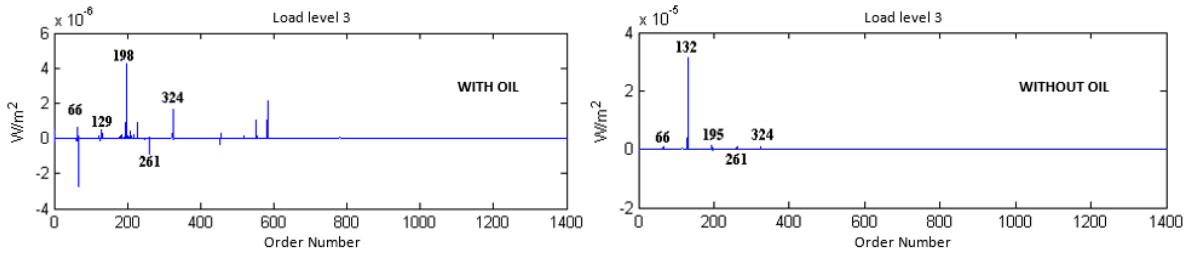

Fig. 13. Intensity spectra comparison on the central grid point with and without lubrication (TSA, 3150 Hz, Speed 2, Load 3).

It can be observed an increase in the spectra maximum amplitude of around one order of magnitude. It is almost exclusively due to the peak related with the third order of the mesh frequency. This is beause the planets have a mesh phase displacement of $2\pi/3$ and then the measured mesh frequency is three times the mesh frequency with only one planet. Besides, any vibratory phenomena related to the teeth contact is augmented because of the lack of damping provided by the oil. Otherwise, the spectra show a clear difference easily identifiable, which could be useful to stablish a warning maintenance parameter.

5.2 Defective planet tooth fault test

In order to generalize the study, a different type of defect was recreated. It consists in a notch in the tooth root of one the planets which decreases its stiffness (Fig. 14). The measurements were limited to the test bench side face. Additionally, the rectangular measuring grid was replaced by a radial one in line with the geometry of the train, as shown on the right handside of Fig. 13.

Fig. 15 and Fig. 16 show the sound intensity spectra under the different combination of operating parameters respectively in normal operation and in operation with a defective planet in the test box. In all the cases, the mesasurement point was the central point of the grid and gearbox. Additionally, Fig. 17 shows the intensity maps for the two said operating conditions. In all cases, the TSA was applied to improve the results.

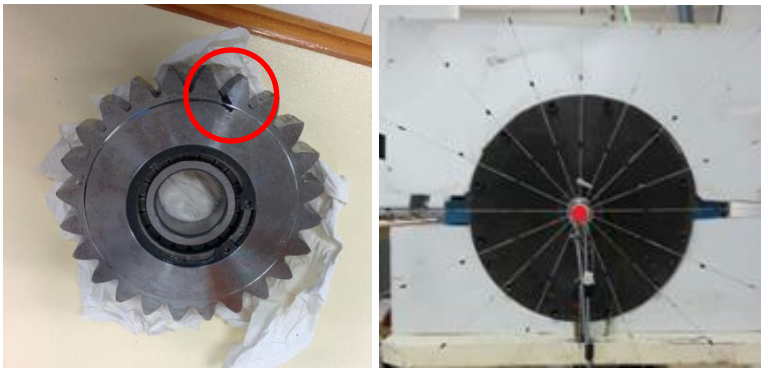

Fig. 14. Notch in the planet and radial measuring grid in side face.

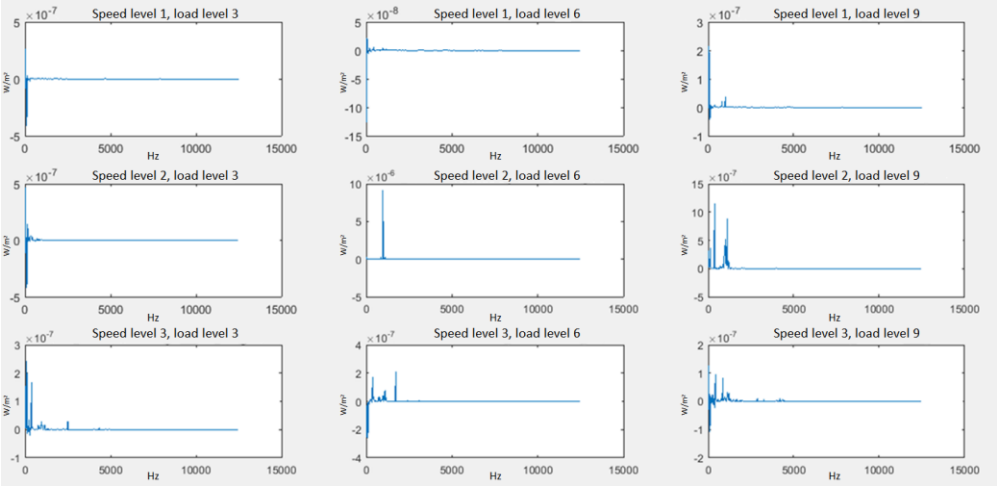

Fig. 15. Sound intensity spectra for test box in normal operation

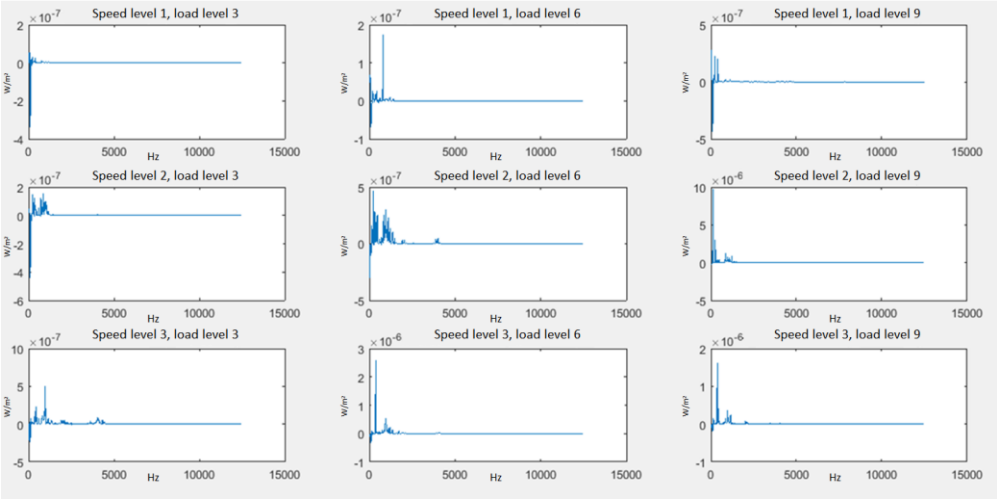

Fig. 16. Sound intensity spectra for test box with defective planet

The defective gearbox spectra show higher amplitude values at all speed levels compared to those of the box under normal conditions. For the box without defect, the spectra have some peaks of much greater amplitude than the rest of the spectrum. However, in the defective box, the spectra are more continuous for the intermediate speed and again show outstanding peaks for the maximum speed. Taking into account that the mesh frequency of the defective tooth is low for any of the speeds tested, it is difficult to see the peaks directly related. Moreover, the lack of rigidity of the defective tooth will cause an overload of the contiguous ones and, therefore, some redistribution of the vibratory energy around the frequency of meshing.

Regarding the intensity maps (Fig 16), the radial grid improves the identification of patterns according to the geometry of the planetary train. In the case of the defective box, these patterns disappear because the defect implies an asymmetry of the set. This lack of symmetry can be used for fault diagnosis, although it is not a simple task. It may require, for instance, the use of image identification techniques for automation within a predictive maintenance system.

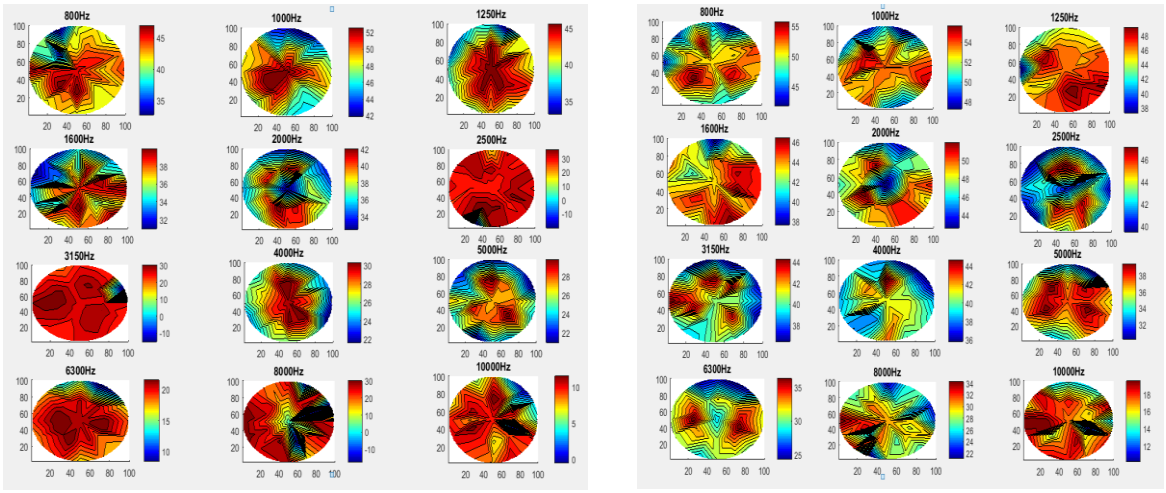

a) b)

Fig. 17. Sound intensity maps for test box a) in normal operation; b) with defective planet.

Figure 16 shows that higher sound intensity levels are achieved in the case with defective planet. Furthermore, especially the intermediate frequency bands, the intensity gradients are also more pronounced, while the higher levels are more concentrated than in the normal operation case.

6. Conclusions

In this study, the use of acoustic measurements of pressure and intensity in the characterization and condition monitoring of planetary gear boxes was assessed. The measurements were carried out on a planetary gearbox installed in a specific test bench. The gearbox was run under normal operating conditions and with two different defects separately. The acoustic results were presented through frequency spectra and intensity maps.

Mesh frequencies are better identified in acoustic pressure spectra than in intensity ones, mainly because the directional nature of the latter attenuates many harmonic components which do not coincide with the axis of the probe. In any case, it is convenient to represent them in orders of the carrier, since, in this way, the harmonics of the meshing frequencies are in the same position, independently of the speed of rotation.

Similar to what happens with vibratory measurements, the synchronous averaging technique has been proven effective in cleaning acoustic measurements of noise unrelated to the gear train.

Intensity maps measured from frontal face are less representative of gearbox condition than those measured from side face as expected due to the movement of the gearbox elements, which is parallel to this face. The intensity maps of the box without defect show radial patterns in line with the geometry and expected noise sources from mid-frequency bands. The use of a radial reference grid helps to distinguish this kind of pattern from lower frequency bands.

The maps from the lack of lubrication condition show a general increase of intensity levels, but no pattern appears. On the other hand, the maps from defective planet tooth condition keep some kind of radial pattern but it cannot be easily related with the defect. Therefore, the application of these maps in condition monitoring is not a straightforward task and it is needed to perform more tests and try different processing techniques, including those of image recognition. However, the measurement of sound intensity in specific external points of the gearbox could be useful to this aim according to the current results. Moreover, the application to systems with a thinner or less closed housing could provide better results. A denser measurement grid could give also better results.

The technique described in this paper is not expected to have, in general, the sensitivity of other similar existing procedures. This is due to two main reasons: (i) the limited frequency sound band and (ii) the use of third octave bands in the analysis of the results. However, the simplicity and quickness of measurements are its main advantages, which can be an asset in, for instance, product verification at the end of the manufacturing process.

Acknowledgments

This work has been supported by project DPI2017-85390-P funded by the Spanish Ministry of Economy, Industry and Competitiveness.

7. References

[1] A. Mihailidis, C. Pupaza. Design Optimization of High Ratio Planetary Systems. Power Transmissions Mechanisms and Machine Science Volume 13, pp. 479-485, Springer Netherlands 2013.

[2] A. Mihailidis, I. Nerantzis, E. Athanasopoulos, Overload capacity of a Wolfrom type planetary system. International Journal of Structural Integrity 2015 vol. 6 issue 5, pp. 636-648.

[3] Nejade, A. On holographic reconstruction without reference: Application to machinery noise and comparison with multi-reference holography approach. Applied Acoustics (2017), 116, pp. 348-356.

[4] Theodossiades, S., De La Cruz, M., Rahnejat, H. Prediction of airborne radiated noise from lightly loaded lubricated meshing gear teeth. Applied Acoustics (2015), 100, pp. 79-86.

[5] Nie, M., Wang, L. Review of condition monitoring and fault diagnosis technologies for wind turbine gearbox. Procedia CIRP (2013), 11, pp. 287-290.

[6] Baydar, N., Ball, A. Detection of gear failures via vibration and acoustic signals using wavelet transform. Mechanical Systems and Signal Processing (2003), 17 (4), pp. 787-804.

[7] Jena, D.P., Panigrahi, S.N., Kumar, R. Multiple-teeth defect localization in geared systems using filtered acoustic spectrogram. Applied Acoustics (2013), 74 (6), pp. 823-833.

[8] Jena, D.P., Panigrahi, S.N. Automatic gear and bearing fault localization using vibration and acoustic signals. Applied Acoustics (2015), 98, art. no. 5572, pp. 20-33.

[9] Anand P., Amandeep S. Gearbox fault diagnosis using acoustic signals, continuous wavelet transform and adaptive neuro-fuzzy inference system. Applied Acoustics (2018), In Press, Available online 27 October 2018

[10] D'Elia, G., Mucchi, E., Cocconcelli, M. On the identification of the angular position of gears for the diagnostics of planetary gearboxes. Mechanical Systems and Signal Processing (2017), 83, pp. 305-320.

[11] A. Kahraman. A theoretical and experimental investigation of modulation sidebands of planetary gear sets. J. Sound. Vib. 323, 677-696

[12] Yi Guo, Tugan Eritenel, Tristan M. Ericson, Robert G. Parker. Vibro-acoustic propagation of gear dynamics in a gear-bearing-housing system. Journal of Sound and Vibration,Volume 333, Issue 22, 2014, pp. 5762-5785.

[13] P. McFadden. A revised model for the extraction of periodic waveforms by time-domain averaging. Mechanical Systems and Signal Processing 1 (1) 1987, pages 83-95.

[14] Mbarek, A., Del Rincon, A.F., Hammami, A., Iglesias, M., Chaari, F., Viadero, F., Haddar, M. Comparison of experimental and operational modal analysis on a back to back planetary gear (2018) 124, pp. 226-247.

[15] Mbarek, A., Hammami, A., Fernandez Del Rincon, A., Chaari, F., Viadero Rueda, F., Haddar, M. Effect of load and meshing stiffness variation on modal properties of planetary gear (2017). Article in Press.

[16] Hammami, A., Fernandez Del Rincon, A., Chaari, F., Santamaria, M.I., Viadero Rueda, F., Haddar, M. Effects of variable loading conditions on the dynamic behaviour of planetary gear with power recirculation (2016) 94, pp. 306-315.

[17] W.J. Atherton, A. Pintz, G. Lewicki. Automated Acoustic Intensity Measurements and the Effect of Gear Tooth Profile on Noise. 1987 Vibrations Conference sponsored by the American Society of Mechanical Engineers Boston, Massachusetts, September 27-30.

[18] Lee, Y., Williams, E.G. Nearfield acoustic holography: I. Theory of generalized holography and the development of NAH Journal of the Acoustical Society of America (1985), 78 (4), pp. 1395-1413.

[19] Albarbar, A., Gu, F., Ball, A.D., Starr, A. Acoustic monitoring of engine fuel injection based on adaptive filtering techniques. Applied Acoustics (2010), 71 (12), pp. 1132-1141.

[20] Tandon, N., Nakra B.C., The application of the sound-intensity technique to defect detection in rolling-element bearings, Applied Acoustics,Volume 29, Issue 3, 1990, pp. 207-217.

[21] S. Gade. Sound Intensity (Instrumentation & Applications). Bruel & Kjaer Technical Review 4, 1982

[22] Fahy, F. Foundations of Engineering Acoustics, pp. 1-443. Elsevier Academic Press. London (2001).

[23] A. Fernandez del Rincon, R. Cerda, M. Iglesias, A. de-Juan, P. Garcia, F. Viadero. Test bench for the analysis of dynamic behavior of planetary gear transmissions. In Advances in Condition Monitoring of Machinery in non-stationary Operations. Lecture Notes in Mechanical Engineering. 2014.

[24] Iglesias, M., Fernandez del Rincon, A., de-Juan, A., Garcia, P., Diez-Ibarbia, A., Viadero, F. Planetary transmission load sharing: Manufacturing errors and system configuration study (2017) 111, pp. 21-38.

[25] Iglesias, M., Fernandez del Rincon, A., de-Juan, A., Diez-Ibarbia, A., Garcia, P., Viadero, F. Advanced model for the calculation of meshing forces in spur gear planetary transmissions (2015) 50 (7), pp. 1869-1894.